TJPS-26096: Original Article

Mapping the impact of polar aprotic solvent on microstructure and dynamic phase transition in glycerol monooleate/ oleic acid system

Marzuka Shoeb Kazi, Mohammed Hassan Dehghan
Department Of Pharmaceutics, Y.b.Chavan College Of Pharmacy, Dr. Rafiq Zakaria Campus, Aurangabad, India

Abstract

Objective: The impact of incorporating a polar aprotic solvent, dimethyl sulfoxide (DMSO) to glycerol monooleate (GMO)/ oleic acid (OA) system was evaluated briefly, on purpose to map its influence on gel microstructure and dynamic phase transition in controlling performance of polyene antifungal drug delivery system.

Methods: An *in-situ* gelling fluid precursor system (IGFPS) exhibiting inverse lyotropic liquid crystalline (LLC) phases was developed by simple solution add-mixture method. Polarized light microscopy (PLM), small angle X-ray scattering (SAXS), Differential scanning calorimeter (DSC) and oscillatory rheological assessments were performed to ascertain microstructural modulations. The developed system was examined for minimum gelling volume, gelling time, swelling behavior, mucoadhesion, *in-vitro* antifungal activity and *in-vitro* drug release.

Results: SAXS study identifies coexistence of Im3m cubic phase with HCP P63/mmc

hexagonal structures. SAXS and DSC data highlight DMSO's unique ability to work both as a kosmotropic or chaotropic solvent and to be a function of its concentration. *In-vitro* antifungal test results point out the concentration of DMSO to be a controlling factor in drug release and diffusion. *In-vitro* drug release kinetic studies reveal most of the gel samples to follow matrix model and anomalous type release as implied by Peppas model.

Conclusion: Finally, the antifungal IGFPS formulated were found to have the required low viscosity, responsive sol–gel phase transition, appreciative mechanical properties and desirable antifungal effect with sustained drug release performance.

Keywords: dimethyl sulfoxide; glycerol monooleate; microstructure; oleic acid; small angle X ray scattering.

Introduction

Dimethyl sulfoxide (DMSO, $(CH_3)_2SO$) is a short amphiphilic moiety, conventionally used as a cryoprotectant, solvent for lipophilic drugs, it is the solvent of choice for the synthesis of sugar ester (used for ice cream production), cell fusogen, and chemical penetration enhancer to deliver active molecules through the skin and into the cell [1, 2]. DMSO interacts with lipids to replace water in the inner region of lipid head groups increasing the area of lipid and decrease its thickness [3]. The hydrophilic group of DMSO interrelates with water and polar head groups of lipids, whereas the two

hydrophobic methyl groups intermingle with the hydrophobic inner membrane region of lipids [4]. Due to its dual character, DMSO occupies the inner interface region and acts as a surfactant to stabilize the presence of water molecules. Lipids such as oleic acid and glycerol monooleate (GMO) have a polar head and a relatively short hydrophobic carbon chain. GMO is categorized as GRAS approved nontoxic, biodegradable and biocompatible material and is also cited in the FDA Inactive Ingredients Guide. Glycerol monooleate was for the first time introduced in 1930, for margarine production, since than is extensively used in food industry as an emulsifier, stabilizer for foams in bread, cakes, margarine, ice creams and chewing gums [5]. Oleic acid (OA) is a monounsaturated fatty acid (triglycerides) component of human diet obtained from animal fats and vegetable oils.

The interaction of DMSO with oleic acid and GMO results in modulation of the microstructure of the lyotropic liquid crystalline system which is formed due to transformation of the sol system to gel phase upon contact with external stimuli like body fluids and excess water. The microstructure formed is primarily controlled by additives in the system and the nature of the drug i.e. hydrophilic or lipophilic. The reversed hexagonal and bicontinuous cubic mesophases are spontaneously formed from the *in-situ* gelling liquid crystal forming system with impetus to an external stimuli. The tortuous networks of aqueous nanochannels formed in these mesophases

partake as gateways for the sustained release of drugs from the gelled liquid crystal structure. In this investigation an *in-situ* gelling system was developed by adding a polyene antifungal agent Nystatin, widely used against susceptible cutaneous and mucocutaneous fungal infections caused by the Candida species as well exhibits a broad spectrum of activity against other fungi such as Aspergillus and Cryptococcus. Interestingly, there are reports that these polyene moiety interact with phospholipids and therefore liposomal formulations have been developed to reduce its toxic effects [6].

In the present study, the impact of incorporating a polar aprotic solvent, DMSO to GMO/OA system was evaluated briefly, on purpose to map its influence on gel microstructure and dynamic phase transition in controlling performance of polyene antifungal drug delivery system.

Materials and methods

Materials

Nystatin was procured as a gift sample from Glenmark Pharmaceuticals, Mumbai. Cithrol GMO-HP-SO-LK was sort as a gift sample obtained from Croda Oleic acid, Dimethyl sulfoxide, methanol, dimethyl formaide and chloroform were acquired from Loba chemie, Mumbai. Dextrose, peptone and agar were purchased from Fisher scientific, India. *Aspergillus fumigatus* (NCIM 902) and *Candida albicans* (ATCC

18804) was procured from National chemical laboratory, Pune. Cellulose acetate membrane pore size 0.45 µm was purchased from Millipore. Goat intestinal mucosa was obtained from local slaughter house.

Formulation of In-situ gelling fluid precursor systems (IGFPS)

The formulation of IGFPS is summarized in Table 1, to prepared by simple add-mixture method, briefly Nystatin (2.23 % w/w) was dissolved in DMSO, the resulting solution was added to oleic acid and vortexed mixed (B-6R-47, Biocraft scientific systems) for 5 minutes for obtaining homogenous solution. The resulting solution was then added to melted (40±2 ◦C) GMO and vortexed mixed for additional 15 minutes. The IGFPS were stored at room temperature until further characterization was performed.

Characterization

In-situ gelling ability and Gelation Time

The minimum solvent (Vm) and minimum time (Tm) required for complete gelation of IGFPS was determined by magnetic stirring method[7]. 1 g of the IGFPS was aliquot into a 5-mL vial; a magnetic bar (10 mm×6 mm) was added into the vial. The temperature was maintained at 37.0±0.5°C and the speed of the magnetic bar was set at 30 rpm. Distilled water (10 µl) was added into the vial each 1 min, until the magnetic bar completely stopped moving due to gelation. For Tm above procedure

was used and excess amount of distilled water was added into the vial, the time required for complete halt of magnetic bar was noted as Tm.

Drug content and pH value of IGFPS

For drug content determination, briefly 1g of formed gel was dissolved in 100 ml of solvent system comprising of methanol: DMF: water (55:15:30) and was evaluated at 306 nm using Shimadzu UV-1600 spectrophotometer. The pH value of IGFPS was determined using Systronics Digital pH meter 335.

Swelling studies

The water uptake of the systems was measured gravimetrically at fixed time intervals, briefly 0.5 g IGFS were weighed on filter paper (40 mm in diameter) soaked in distilled water and positioned on top of a sponge (5 cm x 5 cm x 2 cm) previously soaked in the hydration medium and placed in a petri dish filled with the distilled water to a height of 0.5 cm[8]. This investigational set-up was kept closed. The water uptake was determined as the increase in weight of the sample over time normalized to the initial weight of the dry systems[8]. The data was subjected to mathematical models [9] using the following equations, to affirm the kinetics of swelling whether first order or second order.

$$\mathrm{In}\frac{w_\infty}{w_{\infty-w}} = kt \qquad 1$$

$$\frac{t}{w} = \frac{1}{kw_\infty^2} + \frac{t}{w_\infty} \qquad 2$$

Where, W∞- maximum water uptake, W- water uptake at a time t, (W∞−W) represents the unrealized water uptake, and k is the proportionality constant. For the second order kinetics, the initial rate of swelling is the reciprocal of the y-intercept in the plot of t/W versus t. The reciprocal of the slope indicates W∞, which is the maximum or equilibrium water uptake. The units of W∞ are grams of buffer absorbed per gram of matrix (g/g), and the units of the initial swelling rate are grams of buffer absorbed per gram of dry matrix per hour (g/g h)[10, 11] .

Polarised light microscopy

The hydrated gels were evaluated at 20±0.5◦C, 27±0.5◦C and 37±0.5◦C for its microscopy (Carl Zeiss Jena, Germany) images under 40x magnifications. The samples were inserted between two glass microscope slides and observed with cross polarizers, to ascertain the type of lyotropic liquid crystal mesophase formed on the basis of characteristic textures[12].

Mucoadhesion measurement by tensile strength method

A CT3 Texture Analyzer (Brookfield Engineering, UK) was used for the tensile strength measurements. Fresh goat intestinal mucosa was obtained from a local slaughterhouse. The dissected mucosal pieces were kept in saline solution in an ice bath until tests were performed. The mucosa was fastened to a 10 mm analytical movable probe of the texture analyzer by a rubber ring and the formulation was

located on the lower platform. The system was maintained at 37 ± 1°C by a thermostatic bath. The measurement was triggered to begin as the upper probe encountered a force of 3 mN upon contact with the sample (1g). The probe was kept in contact with no force applied for 60 s, after which it was raised at the speed of 1 mm/s, and the force needed for detachment was estimated. The tensile work, which is proportional to the area under the force–time curve, was used to describe the mucoadhesive characteristics.

Rheological measurements

Rotational and oscillatory rheological tests were performed for formed gel samples using a Kinexus Rheometer (Malveran Instruments Ltd, UK). Rotational and oscillatory tests were performed at 37.0 ± 0.1°C. Rotational tests were used to determine the viscosity and the data were analyzed for type of flow pattern. Oscillatory tests were performed to define the elastic modulus, loss modulus and complex viscosity. The shear rate during the rotational tests ranged from 2 to100 s^{-1}. For oscillatory analysis, first the stress sweep measurements (0.001-10 %) were performed at a constant frequency of 1 Hz in order to determine the linear viscoelastic region. Afterwards, the oscillatory shear measurements were carried out as a function of frequency (0.1–100 Hz) at constant strain of 0.1%.

Small-angle X-ray scattering (SAXS)

Scattering data were obtained by using NANO-Viewer, Rigaku, Japan with 2D Hybrid Pixel Array detector, Cu Kα is used as the radiation source (0.154A˚) from Micro-focus rotating anode X-ray generator operated at a power rating of 40 kV, 30 mA. Samples were subjected to X-ray exposure for 10 minutes with a sample to detector distance set at 800 mm. The measurements were performed at various temperatures i.e. 20°C, 27°C and 37°C with a q range of 0.028 to 0.213 $Å^{-1}$.

Differential Scanning Calorimeter (DSC)

DSC Q 20 (TA Instruments) was used for analyzing the prepared samples. Indium and zinc standards were used for calibration of instrument. A 10±3 mg of hydrated sample was placed in aluminum crucibles separately. The crucibles were equilibrated at 25°C and then the samples were rapidly cooled in liquid nitrogen from 25°C to −25°C, at a rate of 10°C min^{-1}. The samples were held at this temperature for 30 min and then were heated at a rate of 2°C min^{-1} to 50°C. An empty pan was used as reference. The fusion temperatures of the components and the total heat transferred in thermal processes was determined.

In-vitro antifungal activity

The *in-vitro* antifungal activity of the formed gel was evaluated against Aspergillus fumigatus (NCIM 902) and Candida albicans (ATCC 18804). Briefly culture suspension of candida albicans was prepared from fresh cultures (2 day old) grown

on Sabouraud dextrose agar slants, by dispersing one loop full of culture in sterile water 5ml and vortex mixing for 15 s to obtain homogenous suspension. The optical density of the resulting culture was determined by Elico spectro colorimeter CL 153 set at a value 1 at 600nm[13]. Inoculum suspensions of Aspergillus fumigatus were prepared from fresh, mature (3-5 day old) cultures grown on Sabouraud dextrose agar (SDA) slants. The colonies were covered with 5 ml of distilled sterile water. Tween 20 (1%) was added to facilitate the preparation of Aspergillus inocula[14]. The inocula were achieved by carefully rubbing the colonies with a sterile loop; the isolates were then shaken vigorously for 15 s with a vortex mixer and then transferred to a sterile tube [14]. The optical density of the suspensions was measured by UV spectrophotometer (Shimadzu UV-1600) was set as 0.13 at 530 nm[14]. Agar well diffusion method was used to evaluate anti-fungal activity, 1 ml of microbial inoculum was seeded into SDA medium and poured into petri plates, a sterile cork borer of diameter 6 mm were punched aseptically to create a well and gel sample (0.1 g) is added into the well. The plates were incubated for 24 hrs, 27°C (Candida albicans) and 48 hrs, 27°C (Aspergillus fumigatus). The drug release from the prepared gel was compared with standard drug solution of Nystatin prepared in DMF (1000 units/ml).The antimicrobial agent diffuses in the agar medium and inhibits the growth of the microbial strain tested.

In-vitro drug release

In-vitro drug release was evaluated by placing cellulose acetate membrane (0.45 µm) between the donor and the receptor chambers of a Franz diffusion cell. Briefly 1 g of prepared gel was placed on the membrane, the receptor compartment was filled with 50ml Methanol: DMF: water (55:15:30) as the dissolution medium[15], at fixed time interval 1 ml of the sample was withdrawn and replaced by fresh solvent to maintain sink condition. The temperature was maintained at 37°C by circulating water bath. UV Spectrophotometric analyses of aliquots were performed at 306 nm to estimate drug release. The experimental data obtained from drug release experiments were evaluated for drug release kinetics, PCP-Disso-V 2.08 software was used to fit models to the release data. The models were assessed on the basis of correlation coefficient (R^2) to mark the best fit model.

Statistical Analysis

The data were articulated as mean ± S.D. ANOVA followed by post hoc Tukey test (GraphPad Prism 8.0.1) was employed to statistically analyze the data at 95% confidence level.

Results and discussion

In-situ gelling ability (Vm) and gelling time (Tm)

The additives added induce a change in the hydration state of the polar lipid head and

affects the critical packing parameter of the lipid[16-19]. The effect of solvent on the gelling property of IGFPS is given in Table 2. It is observed that increasing the concentration of DMSO and oleic acid had significant effect on the minimum amount of distilled water required for in-situ gelling. High amount of distilled water was required for gelling in case of IGFPS of F2, where as the least amount of solvent was required in formulations F5. Higher concentration of DMSO results in disrupting of water channels [20-22]. Whereas in case of F5 equal proportion of oleic acid and DMSO causes the solvent to partition between both the phases i.e. the lipids and DMSO, thus making the polar heads of lipids easily available for hydration. Table 2 indicates the results obtained for gelling time (Tm). It was found that there was a reverse relationship between the concentration of DMSO and time required for gelling. The gelling time was obtained in the following order for formulations containing higher DMSO content F2>F3>F1>F8>F6, whereas with increase in oleic acid concentration, showed reduction in gelation time F5<F4<F7<F9. Statistical analysis done using ANOVA followed by posthoc Tukey test for Tm reveal that on comparing means of each group with the other showed high significant difference ($p<0.05$, <0.0001) , whereas insignificant difference was seen in case of F4 vs. F5 ($p>0.05$, 0.1043) and F6 vs. F9 ($p>0.05$, 0.9762). In case, of Vm insignificant difference was seen for F7 vs. F9 ($p>0.05$, 0.2233), F4 vs. F7 ($p>0.05$, 0.6063), F4 vs. F9 ($p>0.05$, 0.9970), F3 vs.

F8 ($p>0.05$, 0.9717) and F1 vs. F6 ($p>0.05$, 0.999), while the other groups showed significant difference ($p<0.05$, <0.0001).

pH of the sol and Drug content

pH of the sol and drug content are presented in Table 2. Almost all formulations showed a drug content in the range 99 to 100 %, while the pH of the sol for all formulations was ranged in a value of 5.5±0.11 to 7±0.34.

Swelling studies

The concentration of DMSO in IGFPS played an important role in modulating the microstructure of the formed gel and had a marked effect on rate of swelling. Figure 1 highlights the swelling behavior, it was monitored for a time span of 8 hrs. IGFPS formulations with higher concentration of DMSO higher was its rate of swelling whereas the formulations were in the concentration of oleic acid was higher the rate of swelling was lower. It was markedly observed that formulations F7 and F5 in initial hour showed faster rate of swelling (Figure 1b), but the same declined in later hours and at the end of 8 hours maximum swelling observed was 24% and 22.75% respectively and is found to be dependent on water uptake[10]. The rapid swelling also stands in contour with other studies signifying formation of a viscous cubic or inverted hexagonal phase is a fast process [23-25]. IGFPS F2 exhibited highest rate of swelling i.e.47% at 8hrs. Herein the concentration of DMSO a polar additive was higher which

preferentially lead to formation of lamellar phase thus DMSO had an opposite effect, as compared to oleic acid could also be a reason for higher rate of swelling. Moreover interaction of GMO with oleic acid and subsequent hydration with water results in reversed hexagonal phases whereas interaction of DMSO with high concentration of hydrated GMO results in predominant cubic phase existence [26, 27]. The results for minimum gelation volume also fall in the same line and demonstrate that concentration of DMSO has a significant effect on gelling as seen for swelling ability. Results of statistical analysis point out that insignificant difference was noted ($p>0.05$) on comparing mean of each group with other, however significant difference was seen ($P<0.05$, <0.01) for F2 vs. F4, F2 vs. F5, F2 vs. F7 and F2 vs. F9. Figure 1c, indicates that all formulations followed second order swelling kinetics which is substantive to earlier reported studies [11,25-26].

Polarised light microscopy (PLM)

IGFPS undergo dynamic structural transition *in-situ* to high-viscous gel on exposure to excess water. This change from a less viscous system into a lamellar, bicontinuous cubic structure, or inverted hexagonal phase can be elucidated by the critical packing parameter (CPP)[28, 29]. Figure 2, indicates PLM images at 20°C, all gel formulations except F2 exhibited dark background with no birefringence characteristic of isotropic liquid crystalline mesophase structure and very possible to be a mesomorphic form of

bicontinuous cubic structure whereas F2 gels casted a two phase region, of lamellar reflects presenting partial textures of birefringence pattern typical of maltese cross and black background of cubic phase. PLM images obtained at 25°C and 37°C (Figure 2) exhibits typical dark backgrounds for F1 and F6 highlighting cubic phase, whereas F2 typically shows only maltese cross pattern thus indicating complete phase transformation to lamellar structure, for the rest gel formulations, coexistence of two phase region with the formation of anisotropic structures with specific fan like texture distinctive of reverse hexagonal structure onto a isotropic black background featuring cubic phase.

Mucoadhesion measurement by tensile strength method

Mucoadhesive properties of lyotropic liquid crystalline systems are seen to be dependent on the dehydration of the mucosa and *in-situ* absorption of water. Intestinal mucosa was selected as a model tissue to understand the influence of formulation additives and mesophase formation on mucodhesion. Table 3, highlights the results for mechanical parameters and bioadhesive force of the gel. The findings indicate that formulation F7 had the highest hardness (1274±60mN), compressibility (1.612±0.072 mJ), adhesivness (3.143±0.12mJ), cohesiveness (1.961±0.053) and bioadhesion force (1010.08±50 mN). On comparing the mean values between formulation F5, F7 and F4 significant difference ($p<0.05$) was noted for the mentioned

parameters. The findings indicate that increasing concentration of oleic acid imparted a better adhesiveness and gel strength for F7, whereas the adhesive force of the gels decreased as the oleic acid content exceeded as seen for formulation F4 and F5. As the compactness of the microstructure increases with increase in oleic acid concentration, the lattice parameter value decreases with narrowing of the water channels leads to decline in adhesiveness and gel strength. Our results corroborates to the reported findings[30]. For formulation F2 lower values of hardness (313.8±30mN), compressibility (0.445±0.020mJ), adhesiveness (0.634±0.012 mJ), cohesiveness (1.175±0.025) and bioadhesion force (254.97±15 mN) was obtained. The results for F2 showed significant difference ($p<0.05$) when compared to the means of F7, poor mechanical parameters were obtained due to predominant lamellar microstructuring of the gel due to high content of DMSO and as reported lamellar phases have poor adhesion in comparison to hexagonal and cubic structures[31].

Rheological measurements

Table 4 and Table 5 indicate the results for rotational and oscillatory test respectively. The value $n<1$ proves the system to be Non-Newtonian typically to be pseudoplastic, the oscillatory parameters complex modulus, elastic modulus, viscous modulus and phase angle (tan δ) reported are calculated at a frequency of 1 Hz. As can be seen the formulations where in DMSO concentration was high showed lower values of

consistency index whereas with an increase in concentration of OA a subsequent rise in consistency index was noted. The general performance of G' and G" as a function of frequency at constant strain 0.1% by the gel sample is illustrated in Figure 3. F1, F3, F4, F6, F7 and F9 typically exhibited frequency dependent moduli curve akin to cubic mesophasic structure. Figure 4 depicts G" to be predominate at lower frequencies (< 0.1 Hz not used), while G' is dominant at higher frequencies since no cross over was seen at the frequencies used in this study. The composition of the sample plays a key role in defining the frequency at which the crossover (G' > G") occurs. As the value of G' levels out after an initial increase, G" is constantly reduced with increasing frequencies. All formulations indicated G' to be higher than one order of magnitude over G". The change from a primarily liquid-like behavior to solid with increasing frequency is supplementary reflected by tan δ values ≥ 1 at low frequency, followed by a swift decline at the crossover, and finally reaching out at tan δ values ≤ 0. The curve for F5 showed some atypical behavior the tan δ values decreased with increase in frequency, but at higher frequency the value was >0, the same has been reported elsewhere[32]. It could be due to high provenance of HCP P63/mmc structure. G" and G' were found to increase at higher frequency and so it can be presumed that the crossover might occur at higher frequency. The sample characterized as F2 also showed a markedly different frequency dependent moduli curve quite similar to seen

for cubic to lamellar structures transformation, herein at higher frequency G" sharply shots up and again the crossover occurs at higher frequency, thus exhibiting viscous property at higher frequency value, although the tan δ value were ≤ 0 .

Table 5 highlights least complex modulus for F2 whereas F5 exhibited the highest value for complex modulus. Statistically evaluation for oscillatory test parameters obtained at a frequency of 1 Hz, the results point out no significant differences ($p>0.05$) for F4 vs. F7, F4 vs. F9 and F7 vs. F9, whereas on comparing with F5 all formulations displayed significant difference ($p<0.05$, <0.001).

SAXS measurements

The liquid crystalline gel microstructure although analyzed by PLM could not conclude on the type of mesomorphic cubic and hexagonal structure formed. Hence, SAXS analysis of the samples becomes essential at different temperature to affirm type of mesomorphic structure formed on the basis of miller indices and change in lattice parameter value. We report intriguing polycontinous interfaces of HCP P63/mmc[33, 34] coexisting with Im3m at 25°C and 37°C. Previous studies have reported coexistence of HCP P63/mmc with Fm3m[35]. The coexistence is a function of the concentration of additive and drug moiety, which grounds to negative interfacial curvature. Studies also point to rigid and closely packed mixed films of phospholipid with nystatin[36]. It has been previously reported that DMSO expands Im3m/Pn3m

cubic phase co-existence region in the phase diagram and increases the lattice constant of the Pn3m monoolein cubic phase[26]. Our results were in contrary to the obtained finding, the presence of oleic acid and nystatin could be the reason for the same, although increase of lattice constant value is seen for Im3m cubic phase with increase in DMSO concentration. SAXS analysis was performed on all the gel formulations and diffractograms were taken at various temperatures i.e. 20°C, 25°C and 37°C to ascertain the effect of temperature on phase transformation and change in lattice parameter. Figure 4 indicates the SAXS diffractograms for all formulations at 20°C, it was seen that all gel samples except for F2, exhibited Im3m (√2:√4:√6:√8:√10:√12:√14) a primitive type of cubic phase structure characterized by three interpenetrating continuous networks, whereas for F2 Im3m phase coexisted with lamellar phase Lα (√1:√4:√9:√16). On cooling self-assembled lipid structures at lower temperature, reduction of bilayer curvature occurs which causes increase in lattice parameter [37, 38]. SAXS diffractogram at 25°C is as shown in Figure 5, it highlights them to be sensitive to change in temperature, F2 was seen to stand apart from the rest with distinctive lamellar peak ratios, F1 and F6 demonstrate the presence of only Im3m phase, whereas others indicate coexistence of Im3m with P63/mmc (√4:√16:√1:√2:√5). Complete phase transformation for F2 is seen at 25°C, as the bilayers lack excess area in the form of thermal undulations and less lateral

tension in the bilayers leads to complete transformation to lamellar phase. SAXS diffractogram at 37°C indicate decline in lattice parameter due to shrinking of the water channels with retention in mesophasic structure (Table 6). The findings relate to DMSO unique ability to act both as a kosmotrope (water-structure maker) and chaotrope (water structure breaker) based on its concentration. Finally, the obtained PLM images for all gel samples at respective temperature are in good agreement with SAXS diffractograms.

Differential scanning calorimeter

DSC studies are used in surfactant based microstructures to identify different types and states of water[39, 40]. Phase structure in surfactant system, interaction among polar moieties and water molecule can be concluded briefly through understanding the state of water in the microstructure by subjecting samples to sub zero temperature DSC scanning. Table 7 and Figure 5 depict sharp depression in freezing point of free water characterized by exothermic peak corresponding to crystallization of ice and two endothermic peaks. The first endothermic peak corresponds to melting event for GMO/OA/DMSO interactions whereas the second peak at low temperature indicates melting of interfacial water/bounded water. The interfacial water corresponds to the water entrapped in the highly ordered mesophasic structures. Endothermic peak for free water was not seen for any formulation but exothermic

peak was noted and is ascribed to crystallization of the ice formation in DMSO /water solvent mixture out of the inter-membrane space in the bulk solvent. Minimal changes in endothermic peak temperature were seen for interfacial water in gel samples. The data indicates that the exothermic peak temperature was dependent on DMSO concentration in the gel system and thus F2 indicated high depression in the freezing temperature for crystallization of ice in the binary mixture of DMSO and water. It is reported that at low concentration DMSO is strongly bonded to two water molecules thus rigidifies water structure whereas at higher concentration breaks the water structure this is strongly evident by decrease in coordination number of water which leads to more distorted tetrahedral structure [39-40]. Exothermic peak temperatures obtained for formulations F4, F5, F7 are in corroboration to the above statement. In aggreement to the SAXS data, the DSC results also configure to DMSO's ability to work either as a kosmotropic or chaotropic solvent depending on its concentration. At low concentration it works as water structure maker whereas at high concentration it breaks the water structure and the same is relevantly explained by change in exothermic peak temperature of free water in various gel formulations. The results obtained for DSC studies fall in line to the minimum volume of solvent required for gelation.

In-vitro drug release rate

The release profiles of a water-insoluble drug nystatin, from preformed mesophasic gel formulations was studied to understand the multitude effect of various factors such as addition of components to liquid crystalline phases, lattice parameter and the rate of swelling[24].The results obtain corroborate with such findings as depicted in Figure 6, F2 exhibited maximum rate of swelling showed rapid release of drug i.e. 94% at 8 hrs. Higher concentrations of DMSO in F2 workes as a cosolvent in solubilization of nystatin, the headgroups are better hydrated, thereby forming larger water channels; the same is ascertained by higher lattice parameter value of 144.43. The assessment for F5 indicates lower rate of swelling, thus have a lower drug release of 48 % at the end of 8 hours. In agreement to previous findings[41], following reason may be alluded to understand the observed behavior, nystatin although solubilized, is localized at lipid/water interface, the partitioning into the continuous hydrophobic phase (formed by GMO and oleic acid) and aqueous channels, becomes the rate limiting step for drug release. In addition investigating SAXS analyzes for F5 confirm a bicontinuous cubic phase (Im3m) with an interstice of inverted hexagonal phase [HCP (P63/mmc)] structure. For F5 the lattice parameter ratio of Im3m/HCP (P63/mmc) at 37°C also governed the drug release pattern. F5 exhibited a ratio of 1.295 whereas for F4 and F7 displayed a ratio value of 1.24 and 1.23 respectively. Thus it can be concluded that an inverse relationship exist between the lattice

parameter ratio and drug release, as the ratio increases the drug release decreases. Statistical evaluation revealed insignificant difference among F4, F5 and F7 ($p>0.05$,>0.999), whereas significant difference was noted on comparing means of F4, F5 and F7 against means of F2 ($p<0.05$, <0.03). Thus clarifies the effect of DMSO as solubilizing cosolvent at high concentration and its role in modulating microstructure, thus controlling the release of drug.

The drug release data was subjected to kinetic modeling, the results are presented in Table 8. It is revealed that almost all formulation showcased matrix type of release pattern except for F4, F5 and F7 indicated peppas model of release pattern. Thus identifies that LLC phases do not follow simple diffusion or erosion, and a thus anomalous ($0.45<n<0.89$) mechanisms is involved.

In-vitro antifungal activity

The *in-vitro* antifungal activity of the formulated IFGPS was evaluated to ascertain its efficacy against Aspergillus fumigatus and Candida albicans. *In-vitro* antifungal activity was also performed to substantiate the in-vitro drug releasing ability of gel formulations. Figure 7 is the representation of the zone of inhibition (mm) for IFGPS and standard Nystatin drug solution. Concentration of DMSO played a crucial role in controlling *in-vitro* antifungal activity; IFGPS F2 exhibited a zone of inhibition of 18mm, 17mm against Candida albicans and Aspergillus fumigatus respectively. The

standard drug solution in DMSO was used as control to compare against the formulated IFGPS. In comparison to the standard drug solution, formulation F2 showed no significant difference ($p > 0.05$, 0.3546), whereas for all the other IFGPS significant difference ($p < 0.0001$) was seen. Oleic acid has mitigating role on the release of nystatin, increase in its concentration lead to decline in the zone of inhibition and this could be due to higher partioning of the drug in to oil phase and being retained either at oil water interface or being bonded to the lipophilic groups of GMO or oleic acid, thus unable to be released out of the matrix. On comparing formulations F4, F5 and F7 against the mean values of F2 significant difference ($p < 0.0001$) was noted, whereas on comparing mean of F4, F5 and F7 amongst each other no significant difference ($p > 0.05$, 0.1229, > 0.99) was obtained. The results are in agreement to the data obtained for *in-vitro* drug release. Moreover the matrices of formulation F5, F4 and F7 did reveal an increase in the zone of inhibition on examining after 48 hours in a range of 2±0.08 mm, thus bear out to be sustained release matrices.

Conclusion

Results of this work revealed that IGFPS containing GMO/OA/DMSO could be used for sustaining the release of polyene antifungal agent, Nystatin. The impact of incorporating a polar aprotic solvent had a divergent effect on modulation of the gel

microstructure which ultimately improved the performance magnitude of the delivery system. The IGFPS formed various mesophasic structures like lamellar (Lα), bicontinuous cubic Im3m, as well coexistence of Im3m with hexagonal HCP P63/mmc was affirmed by SAXS and polarized optical microscopy were. DSC and SAXS studies highlight DMSO's ability to work either as a kosmotropic or chaotropic solvent, to be a function of its concentration. Rheological and oscillatory assessment confirmed all samples to show shear thinning behavior, the gels show frequency dependent rheograms of entirely elastic nature G' > G". Texture analysis results underline the presence of requisite mechanical and mucoadhesive properties.

Finally, an *in-vitro* antifungal activity and an *in-vitro* drug release kinetic study proved that the F7, IGFPS containing nystatin has the suitable controlled release property required for an effective mucoadhesive sustain release delivery system. *In-vivo* and stability studies are essential to substantiate the obtained findings, and the model needs to be studied for specific route of administration.

Declaration of interest

The authors report no conflicts of interest. The authors alone are responsible for the content and writing of this article.

Acknowledgements

The authors are thankful to; Glenmark Pharmaceuticals, India for providing Nystatin

as gift sample, Croda, India for bequesting Cithrol GMO HP-SO-(LK). We are highly obliged to Malveran, India for offering technical support for oscillatory analysis.

References

1. Kligman AM. Topical pharmacology and toxicology of dimethyl sulfoxide. Jama. 1965;193:796-804.
2. Vignes R. Dimethyl sulfoxide (DMSO), A “new” clean, unique, superior solvent. Annual Meeting. Washington, DC.; 2000.
3. Yu ZW, Quinn PJ. The effect of dimethyl sulphoxide on the structure and phase behaviour of palmitoleoylphosphatidylethanolamine. Biochimica et biophysica acta. 2000;1509(1-2):440-50.
4. de Menorval MA, Mir LM, Fernandez ML, Reigada R. Effects of dimethyl sulfoxide in cholesterol-containing lipid membranes: a comparative study of experiments in silico and with cells. PloS one. 2012;7(7):e41733.
5. Milak S, Zimmer A. Glycerol monooleate liquid crystalline phases used in drug delivery systems. International journal of pharmaceutics. 2015;478(2):569-87.
6. Ng AW, Wasan KM, Lopez-Berestein G. Development of liposomal polyene antibiotics: an historical perspective. Journal of pharmacy & pharmaceutical sciences : a publication of the Canadian Society for Pharmaceutical Sciences, Societe canadienne des sciences pharmaceutiques. 2003;6(1):67-83.
7. Chen Y, Liang X, Ma P, Tao Y, Wu X, Wu X, et al. Phytantriol-based in situ liquid crystals with long-term release for intra-articular administration. AAPS PharmSciTech. 2015;16(4):846-54.
8. MH GD, Marzuka M. Lyophilized Chitosan/xanthan Polyelectrolyte Complex Based Mucoadhesive Inserts for Nasal Delivery of Promethazine Hydrochloride. Iranian journal of pharmaceutical research : IJPR. 2014;13(3):769-84.
9. Schott H. Kinetics of swelling of polymers and their gels. Journal of pharmaceutical sciences. 1992;81(5):467-70.
10. Souza C, Watanabe E, Borgheti-Cardoso LN, De Abreu Fantini MC, Lara MG. Mucoadhesive system formed by liquid crystals for buccal administration of poly(hexamethylene biguanide) hydrochloride. Journal of pharmaceutical sciences. 2014;103(12):3914-23.
11. Lee J, Choi SU, Yoon MK, Choi YW. Kinetic characterization of swelling of liquid crystalline phases of glyceryl monooleate. Archives of pharmacal research. 2003;26(10):880-5.
12. Rosevear FB. The microscopy of the liquid crystalline neat and middle phases of soaps and synthetic detergents. Journal of the American Oil Chemists' Society.

1954;31(12):628-39.
13. Mitchell BM, Wu TG, Jackson BE, Wilhelmus KR. Candida albicans strain-dependent virulence and Rim13p-mediated filamentation in experimental keratomycosis. Investigative ophthalmology & visual science. 2007;48(2):774-80.
14. Petrikkou E, Rodriguez-Tudela JL, Cuenca-Estrella M, Gomez A, Molleja A, Mellado E. Inoculum standardization for antifungal susceptibility testing of filamentous fungi pathogenic for humans. Journal of clinical microbiology. 2001;39(4):1345-7.
15. Fernandez-Campos F, Clares Naveros B, Lopez Serrano O, Alonso Merino C, Calpena Campmany AC. Evaluation of novel nystatin nanoemulsion for skin candidosis infections. Mycoses. 2013;56(1):70-81.
16. Fong WK, Hanley T, Boyd BJ. Stimuli responsive liquid crystals provide 'on-demand' drug delivery in vitro and in vivo. Journal of controlled release : official journal of the Controlled Release Society. 2009;135(3):218-26.
17. Kwon TK, Kim JC. Monoolein cubic phase containing acidic proteinoid: pH-dependent release. Drug development and industrial pharmacy. 2011;37(1):56-61.
18. Negrini R, Mezzenga R. pH-responsive lyotropic liquid crystals for controlled drug delivery. Langmuir : the ACS journal of surfaces and colloids. 2011;27(9):5296-303.
19. de Campo L, Yaghmur A, Sagalowicz L, Leser ME, Watzke H, Glatter O. Reversible phase transitions in emulsified nanostructured lipid systems. Langmuir : the ACS journal of surfaces and colloids. 2004;20(13):5254-61.
20. Cowie JMG, Toporowski PM. Association in the binary liquid system dimethyl sulphoxide – water. Canadian Journal of Chemistry. 1961;39(11):2240-3.
21. Ur-Rehman T, Tavelin S, Grobner G. Effect of DMSO on micellization, gelation and drug release profile of Poloxamer 407. International journal of pharmaceutics. 2010;394(1-2):92-8.
22. Watase M NK. Effects of pH and DMSO content on the thermal and rheological properties of high methoxyl pectin-water gels. Carbohydrate Polymers. 1993;20(3):175-81.
23. Lara MG, Bentley MV, Collett JH. In vitro drug release mechanism and drug loading studies of cubic phase gels. International journal of pharmaceutics. 2005;293(1-2):241-50.
24. Rizwan SB, Hanley T, Boyd BJ, Rades T, Hook S. Liquid crystalline systems of phytantriol and glyceryl monooleate containing a hydrophilic protein: Characterisation, swelling and release kinetics. Journal of pharmaceutical sciences. 2009;98(11):4191-204.
25. Chang CM, Bodmeier R. Swelling of and drug release from monoglyceride-based drug delivery systems. Journal of pharmaceutical sciences. 1997;86(6):747-52.

26. Abe S, Takahashi H. A comparative study of the effects of dimethylsulfoxide and glycerol on the bicontinuous cubic structure of hydrated monoolein and its phase behavior. Chemistry and physics of lipids. 2007;147(2):59-68.
27. Conn CE, Ces O, Mulet X, Finet S, Winter R, Seddon JM, et al. Dynamics of structural transformations between lamellar and inverse bicontinuous cubic lyotropic phases. Physical review letters. 2006;96(10):108102.
28. Mulet X, Boyd BJ, Drummond CJ. Advances in drug delivery and medical imaging using colloidal lyotropic liquid crystalline dispersions. Journal of colloid and interface science. 2013;393:1-20.
29. Hartnett TE, Ladewig K, O'Connor AJ, Hartley PG, McLean KM. Size and Phase Control of Cubic Lyotropic Liquid Crystal Nanoparticles. The Journal of Physical Chemistry B. 2014;118(26):7430-9.
30. Oyafuso MH, Carvalho FC, Takeshita TM, De Souza ALR, Araujo DR, Merino V, et al. Development and In Vitro Evaluation of Lyotropic Liquid Crystals for the Controlled Release of Dexamethasone. Polymers. 2017;9(8).
31. Evenbratt H, Ström A. Phase behavior, rheology, and release from liquid crystalline phases containing combinations of glycerol monooleate, glyceryl monooleyl ether, propylene glycol, and water. RSC Advances. 2017;7(52):32966-73.
32. Schröder-Turk GE, Varslot T, de Campo L, Kapfer SC, Mickel W. A Bicontinuous Mesophase Geometry with Hexagonal Symmetry. Langmuir : the ACS journal of surfaces and colloids. 2011;27(17):10475-83.
33. Shearman GC, Tyler AI, Brooks NJ, Templer RH, Ces O, Law RV, et al. A 3-D hexagonal inverse micellar lyotropic phase. Journal of the American Chemical Society. 2009;131(5):1678-9.
34. Soni SS, Brotons G, Bellour M, Narayanan T, Gibaud A. Quantitative SAXS analysis of the P123/water/ethanol ternary phase diagram. The journal of physical chemistry B. 2006;110(31):15157-65.
35. Chen Z, Jiang Y, Dunphy DR, Adams DP, Hodges C, Liu N, et al. DNA translocation through an array of kinked nanopores. Nature materials. 2010;9(8):667-75.
36. Hac-Wydro K, Dynarowicz-Latka P. Interaction between nystatin and natural membrane lipids in Langmuir monolayers--the role of a phospholipid in the mechanism of polyenes mode of action. Biophysical chemistry. 2006;123(2-3):154-61.
37. Borné J, Nylander T, Khan A. Phase Behavior and Aggregate Formation for the Aqueous Monoolein System Mixed with Sodium Oleate and Oleic Acid. Langmuir : the ACS journal of surfaces and colloids. 2001;17(25):7742-51.
38. Gurfinkel J, Aserin A, Garti N. Interactions of surfactants in nonionic/anionic

reverse hexagonal mesophases and solubilization of α-chymotrypsinogen A Colloids and Surfaces A: Physicochemical and Engineering Aspects. 2011;392(1):322-8.
39. Shashkov SNK, M. A.; Tioutiounnikov, S. N.; Kiselev, A. M.; Lesieur, P. The study of DMSO/water and DPPC/DMSO/water system by means of the X-Ray, neutron small-angle scattering, calorimetry and IR spectroscopy. Physica B: Physics of Condensed Matter. 1999;271(1):184-91.
40. Yaghmur A RM, Larsen SW. In situ forming drug delivery systems based on lyotropic liquid crystalline phases : structural characterization and release properties. Journal of Drug Delivery Science and Technology. 2013;23(4):325-32.
41. Mei L, Huang X, Xie Y, Chen J, Huang Y, Wang B, et al. An injectable in situ gel with cubic and hexagonal nanostructures for local treatment of chronic periodontitis. Drug delivery. 2017;24(1):1148-58.
42. Patil SS, Venugopal E, Bhat S, Mahadik KR, Paradkar AR. Exploring Microstructural Changes in Structural Analogues of Ibuprofen-Hosted In Situ Gelling System and Its Influence on Pharmaceutical Performance. AAPS PharmSciTech. 2015;16(5):1153-9.

Tables:

Table 1 Formulation of IGFPS

Formulation	Oleic acid: DMSO (%w/w)
F1	1:3
F2	1:5
F3	1:4
F4	3:4
F5	1:1
F6	3:5
F7	2:3
F8	2:5
F9	1:2

*GMO was added quantity sufficient to 100%w/w

Table 2 Minimum volume of solvent for gelation, gelation time and pH

Formulation	Vm (µl)	Water (%w/w)	Tm (secs)	pH	Drug content (%)
F1	120±2.51	10.86±0.75	145±5	6.2±0.21	98.72±0.05
F2	180±1.81	15.51±1.15	180±2.88	7±0.34	99.10±0.01
F3	150±2.88	13.15±0.95	165±3	6.6±0.12	98.55±0.02
F4	90±2.51	8.33±0.5	75±5	6.3±0.15	99.05±0.07
F5	70±2	6.66±0.4	60±4	5.5±0.11	98.82±0.03
F6	120±4.04	10.9±0.8	105±2.88	6.7±0.09	99.32±0.01

F7	90±5.77	8.4±0.6	90±5	5.8±0.17	99.5±0.015
F8	150±5	13.15±1.02	120±5	6.8±0.12	98.67±0.04
F9	100±5.17	9.25±0.75	100±1.88	6.4±0.13	99.18±0.025

(Mean± SD, n=3)

Table 3 Mechanical properties and bioadhesive force of preformed gel formulations

Formulation	Mechanical parameters (n=3)				
	Hardness (mN)	Compressibility (mJ)	Adhesiveness (mJ)	Cohesiveness (dimensionless)	Work of Bioadhesion (mN)
F1	480±40	0.533±0.025	1.111±0.018	1.495±0.030	441.29±20
F2	313.8±30	0.405±0.020	0.634±0.012	1.175±0.025	254.97±15
F3	333.8±20	0.486±0.015	0.678±0.015	1.294±0.020	313.81±12
F4	1002.08±50	1.452±0.022	2.943±0.075	1.816±0.021	935.49±30
F5	657.04±25	1.256±0.025	2.413±0.022	1.682±0.025	539.36±25
F6	363.84±15	0.824±0.015	1.323±0.017	1.492±0.028	342.65±10
F7	1245.44±60	1.712±0.072	3.143±0.12	1.961±0.053	1010.08±50
F8	345.199±18	0.674±0.013	0.956±0.005	1.323±0.025	304.006±14
F9	382.039±16	1.034±0.012	1.338±0.011	1.582±0.021	383.61±20

(Mean± SD, n=3)

Table 4 Rheological parameters of IGFPS sol and preformed gel

Formulation	Viscosity of sol (Pa.s)	n	k (Pa.s)
F1	0.17±0.001	0.0925±0.01	13.5±0.14
F2	0.103±0.0011	0.08612±0.02	10.5±0.21
F3	0.15±0.002	0.09147±0.03	13.1±0.25
F4	0.449±0.015	0.1467±0.005	450.87±1.57
F5	0.555±0.018	0.1598±0.001	571.89±1.25
F6	0.1928±0.0012	0.1102±0.032	50.5±0.1
F7	0.3899±0.002	0.1246±0.004	341.87±1.11
F8	0.1684±0.0013	0.09695±0.01	30.2±0.5
F9	0.3599±0.001	0.099±0.012	138.18±1.02

(Mean± SD, n=3)

Table 5 Oscillatory test parameters of preformed gels at a frequency of 1Hz

Formulation	tanδ	Complex modulus (Pa) G*	Elastic modulus (Pa) G'	Viscous modulus (Pa) G"

F1	14.69	5.76 x10^4	6.55 x10^4	1.71 x10^3
F2	9.13	1.76 x10^4	2.95 x10^4	4.8 x10^3
F3	11.36	3.12 x10^4	3.06 x10^4	6.13 x10^3
F4	19.64	7.68 x10^4	7.23 x10^4	2.58 x10^4
F5	13.91	1.35 x10^5	1.31 x10^5	3.8 x10^4
F6	16.91	1.10 x10^5	9.71 x10^4	2.95 x10^4
F7	17.2	8.3 x10^4	7.96 x10^4	2.47 x10^4
F8	15.84	5.22 x10^4	5.02 x10^4	1.43 x10^4
F9	15.9	7.32 x10^4	7.04 x10^4	2.00 x10^4

(mean, n=3)

Table 6 Lattice parameter, microstructure and lattice ratio of preformed gel samples at 20°C, 27°C and 37°C

Temp.	20°C			27°C			37°C		
Gel	α (A^0)	Lattice ratio	Structure	α (A^0)	Lattice ratio	Structure	α (A^0)	Lattice ratio	Structure
F1	94.28 ±0.611	----	Im3m,Q^{229}	91.32 ±0.39	----	Im3m, Q^{229}	91.32±0.85	----	Im3m Q^{229}
F2	157.85±0.086 104.53±	1.509	Lamellae, Lα Im3m,Q^{229}	150.43±0.825	----	Lamellae Lα	144.43±0.83	----	Lamellae Lα
F3	99.54 ±0.889	----	Im3m,Q^{229}	98.19 ±0.687 84.3±0.513	1.164	Im3m,Q^{229} HCP (P63/mmc)	94.18±0.57 81.64±0.826	1.15	Im3m,Q^{229} HCP (P63/mmc)
F4	84.99 ±1.15	----	Im3m,Q^{229}	83.33 ±0.577 64.75 ±0.507	1.28	Im3m,Q^{229} HCP (P63/mmc)	80.274±0.72 64.33±0.69	1.24	Im3m,Q^{229} HCP (P63/mmc)
F5	89.03 ±1	----	Im3m,Q^{229}	88.86 ±1.037 67.35 ±0.7	1.319	Im3m Q^{229} HCP (P63/mmc)	80.52±1.26 62.13±0.618	1.295	Im3m,Q^{229} HCP (P63/mmc)
F6	88.06 ±0.97	----	Im3m,Q^{229}	84±0.577	----	Im3m,Q^{229}	84.6±0.923	----	Im3m,Q^{229}

	0								
F7	84.9±0.802	----	Im3m,Q^{229}	82.57±0.906 66.02±0.59	1.25	Im3m,Q^{229} HCP (P63/mmc)	79.11±1.06 64.14±0.621	1.23	Im3m,Q^{299} HCP (P63/mmc)
F8	93.23±0.577	----	Im3m,Q^{229}	92.67±0.964 82.07±0.558	1.12	Im3m,Q^{229} HCP (P63/mmc)	89.4±0.635 80.6±0.808	1.109	Im3m,Q^{229} HCP (P63/mmc)
F9	88.21±0.512	----	Im3m,Q^{229}	87±0.577 70.16±0.628	1.24	Im3m, Q^{229} HCP (P63/mmc)	83±0.57 68.57±0.794	1.211	Im3m,Q^{229} HCP (P63/mmc)

(Mean± SD, n=3)

Table 7 Endothermic and exothermic events their peak temperature and enthalpy of preformed gel samples

Formulation	Endothermic peak temperature (^{0}C)		Enthalpy (W/g) for endothermic peaks		Exothermic peak temperature (^{0}C)	Enthalpy (W/g) for exothermic peak
	Interfacial water	Non water melting events	Interfacial water	Non water melting events	Free water	Free water
F1	-12.40	15.68	-0.9272	-1.16	-6.95	0.8507
F2	-16.55	12.83	-0.7723	-1.36	-12.88	0.9938
F3	-15.37	14.73	-0.7966	-1.46	-10.86	0.8696
F4	-15.48	11.65	-1.042	-1.103	-5.12	0.2856
F5	-16.08	11.41	-0.9168	-1.052	-5.05	0.2587
F6	-15.84	15.68	-0.6651	-1.276	-11.09	0.9765
F7	-13.94	12.83	-1.253	-1.327	-6.35	0.8252
F8	-15.72	11.65	-1.049	-1.14	-10.16	0.9126
F9	-15.25	13.19	-1.025	-1.231	-9.856	0.9838

Table 8 Drug release kinetics of the gelled samples

Formulation code	R^2 value					Best fit model	Parameters for Korsemeyer Peppas equation	
	Zero order	First order	Matrix	Peppas	Hixson Crowell		k	n
F1	0.9295	0.5151	0.9929	0.9898	0.9585	Matrix	3.0918	0.52103
F2	0.9031	0.4295	0.9871	0.9174	0.9761	Matrix	6.4823	0.4572
F3	0.9445	0.5039	0.9984	0.9975	0.9797	Martix	3.8208	0.5069
F4	0.9802	0.6651	0.9784	0.9971	0.9873	Peppas	1.1058	0.6255
F5	0.9798	0.6971	0.9852	0.9928	0.9891	Peppas	0.6921	0.6691
F6	0.9327	0.5629	0.9933	0.9912	0.9444	Matrix	2.7079	0.5063
F7	0.9783	0.6681	0.9791	0.9951	0.9862	Peppas	1.1009	0.6391
F8	0.8666	0.5029	0.9781	0.9746	0.9333	Matrix	3.2506	0.4752
F9	0.9265	0.5776	0.9965	0.9929	0.9712	Matrix	1.8137	0.5830

Figures

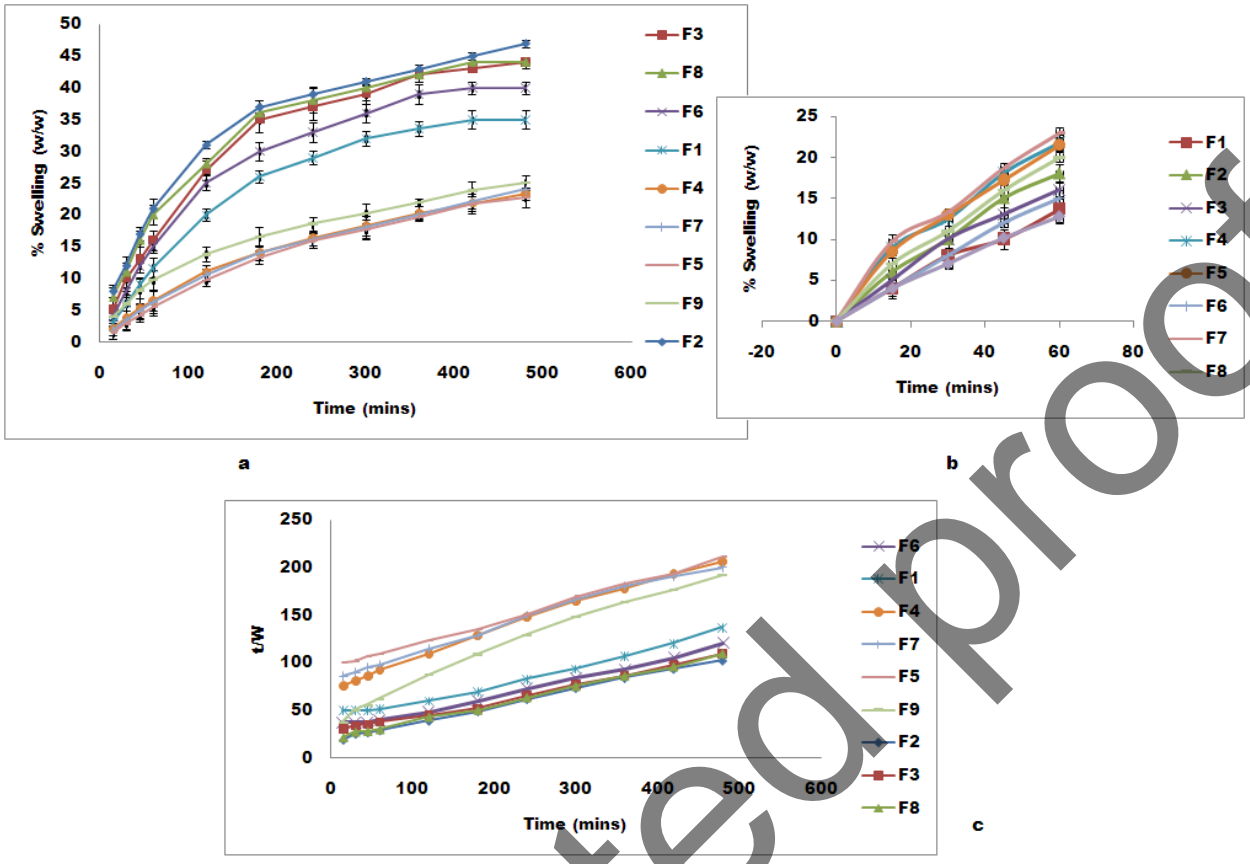

Figure 1. (a) Plots of the percentage increase in the weight as a function of time when placed in excess of water (b) Plots of percentage increase in weight in the initial hour when placed in excess of water(c) Plots of swelling kinetics of different formulation according to second order kinetics

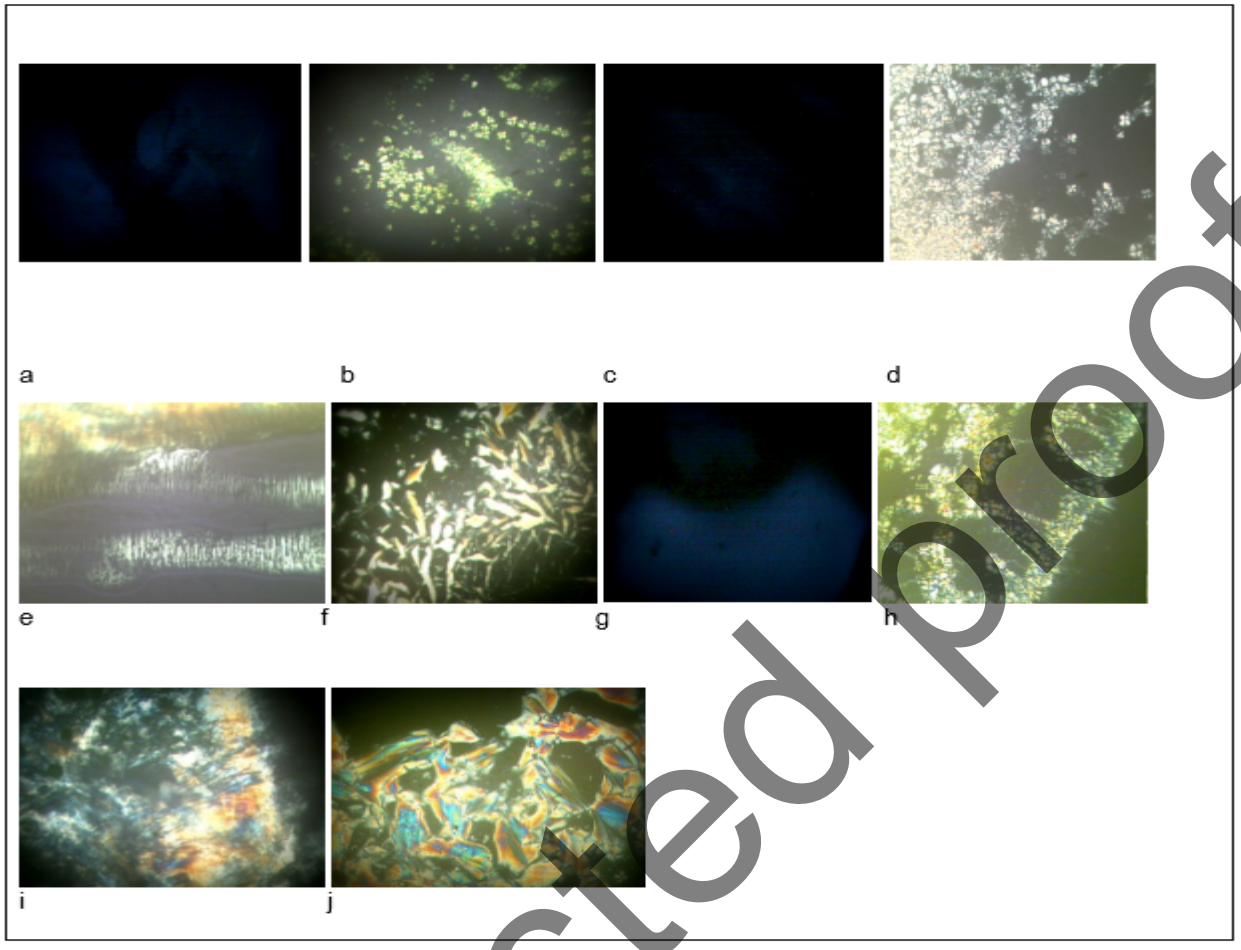

Figure 2.(a) F1, F6, F3 cubic phase at 20^0C and 27^0C (b) F2 cubic and lamellar phase at 20^0C (c) F4, F5, F7, F8, F9 cubic phase at 20^0C (d) F2 lamellar phase 27^0C (e). F3, F8 cubic and hexagonal phase at 27^0C (f) F4, F5, F7, F9 cubic and hexagonal phase at 27^0C (g) F1, F6 cubic phase at 37^0C (h) F2 lamellar phase at 37^0C (i) F3, F8 cubic and hexagonal phase at 37^0C (j) F4, F5, F7, F9 cubic and hexagonal phase at 37^0C

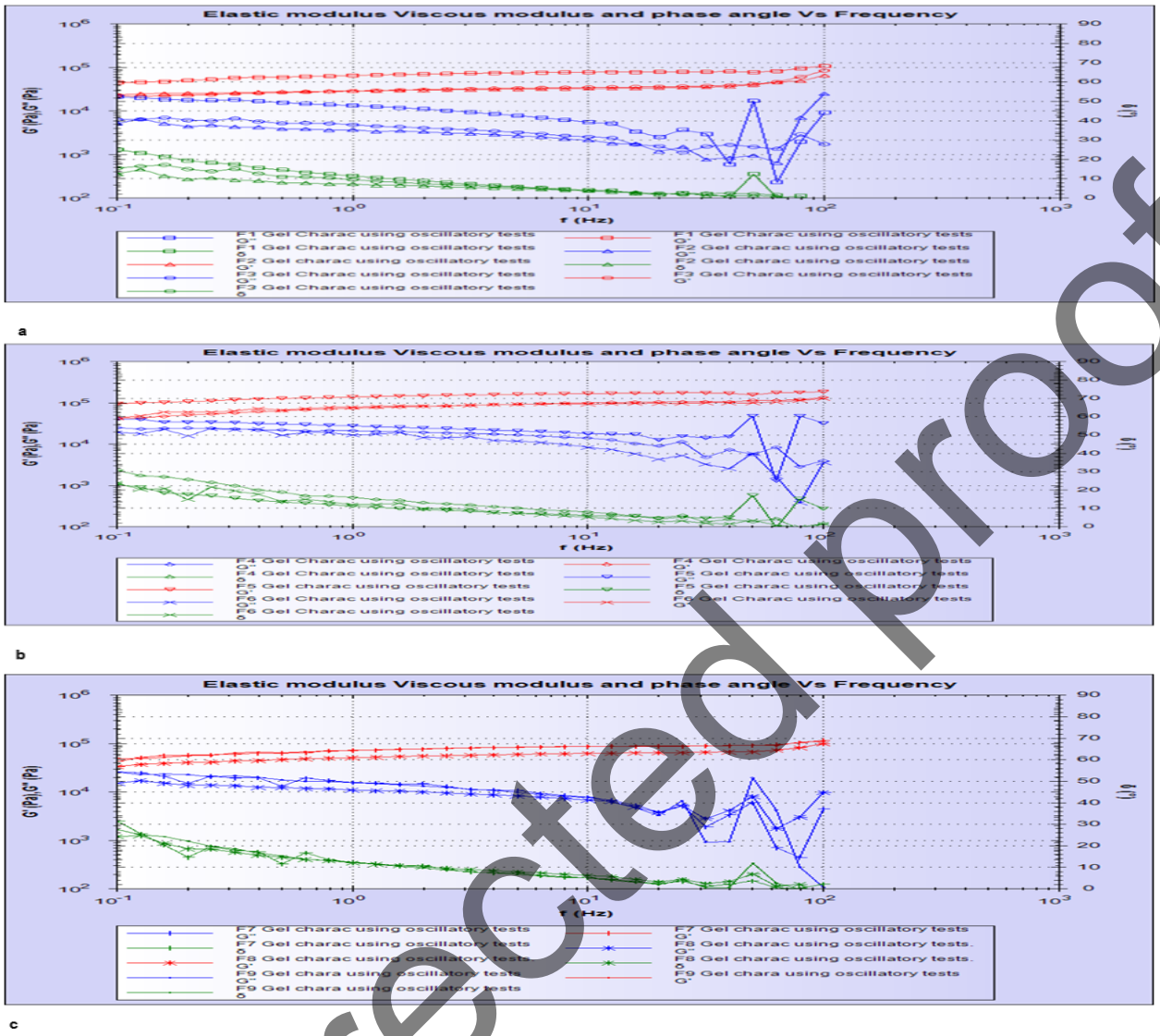

Figure 3.(a) elastic modulus, viscous modulus and phase angle vs. frequency for F1,F2,F3(b) elastic modulus, viscous modulus and phase angle vs. frequency for F4,F5,F6 (c) elastic modulus, viscous modulus and phase angle vs. frequency for F7,F8,F9

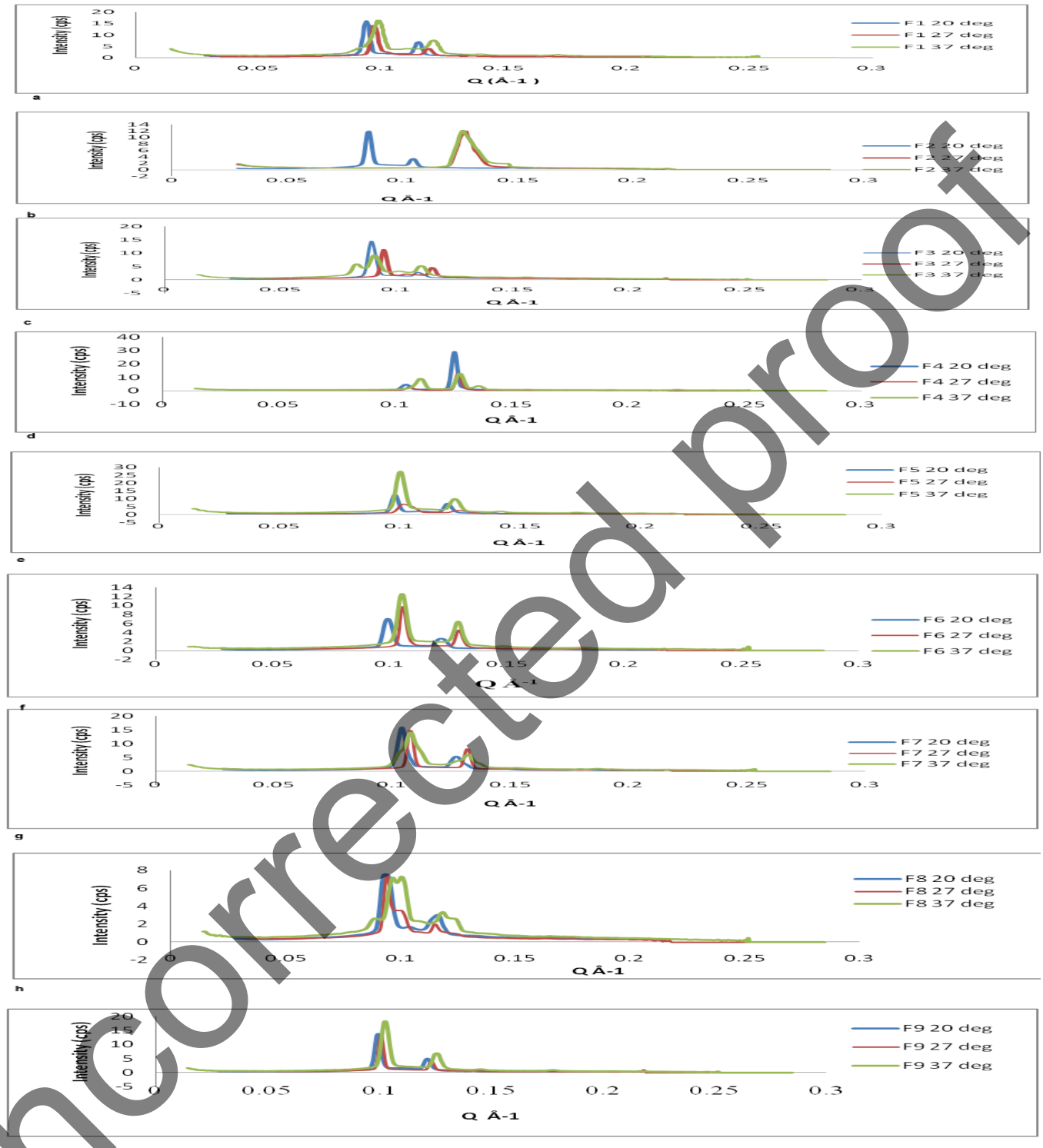

Figure 4. SAXS profile of preformed gel samples at 20^0C, 27^0C and 37^0C (a) F1 (b) F2 (c) F3 (d) F4 (e) F5 (f) F6 (g) F7 (h) F8 (i) F9

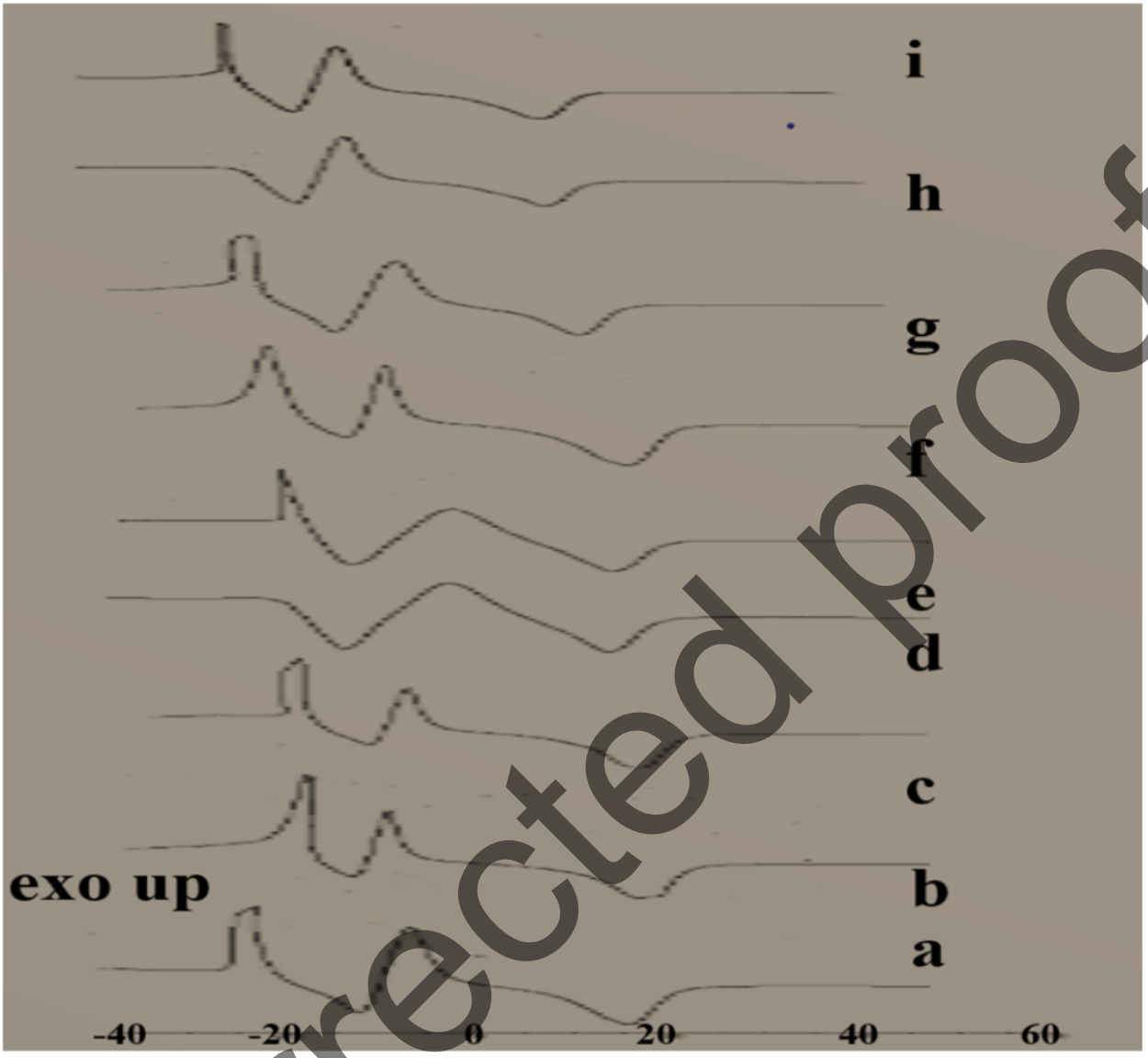

Figure 5. DSC thermograms of preformed gel samples (a) F1 (b) F2 (c) F3 (d) F4 (e) F5 (f) F6 (g) F7 (h) F8 (i) F9

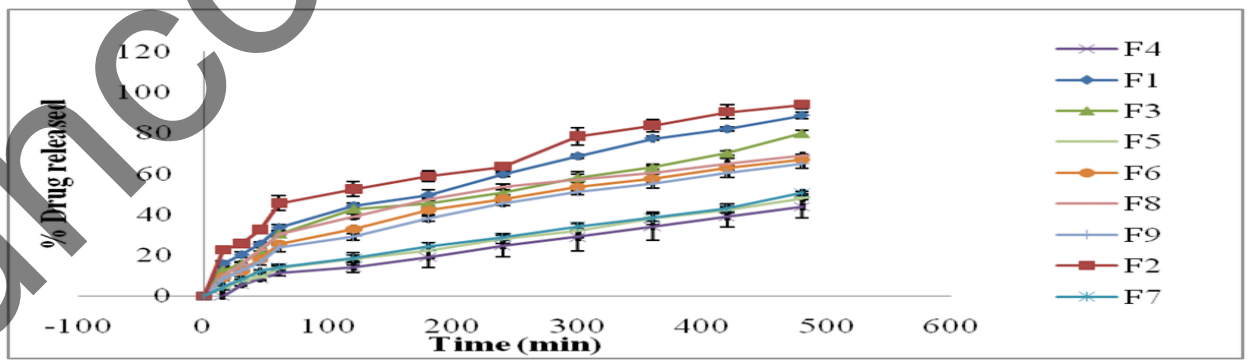

Figure 6. % Drug released vs. time profile of gelled samples

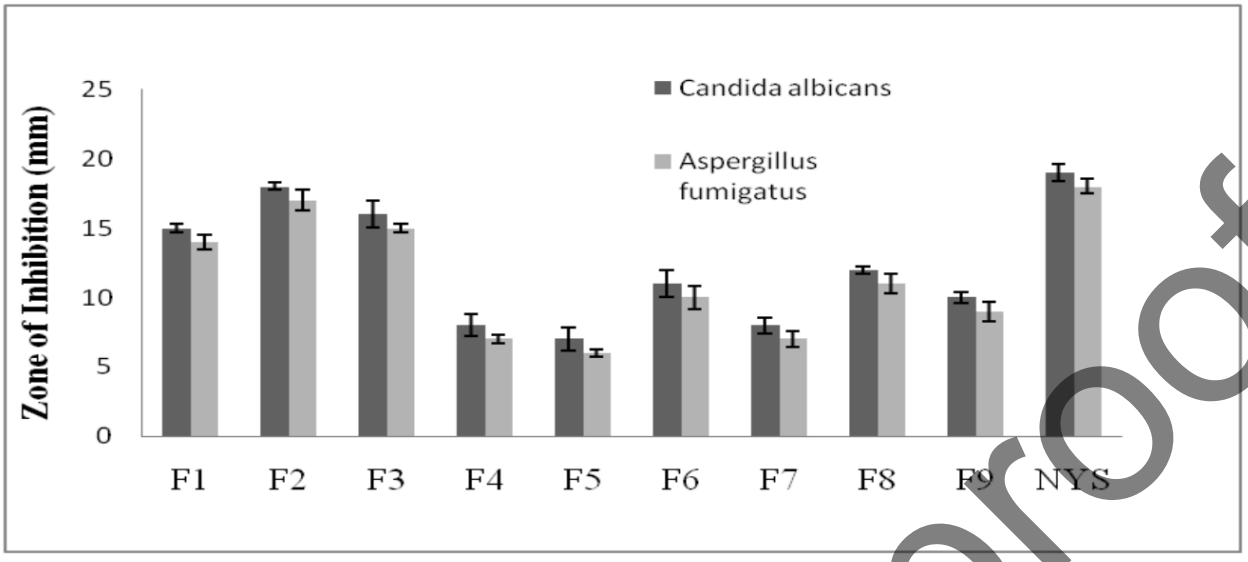

Figure 7. Zone of inhibition of gel samples obtained against Aspergillus fumigatus and Candida albicans